

Refereed Proceedings

*The 13th International Conference on
Fluidization - New Paradigm in Fluidization
Engineering*

Engineering Conferences International

Year 2010

CHARACTERIZATION OF
TURBULENT REGIME BEHAVIOR
IN THE DILUTE ZONE OF A
CIRCULATING FLUIDIZED BED
RISER

Abdelghafour Zaabout*

René Occelli‡

Hervé Bournot†

Bousselham Kharbouch**

*IUSTI Technopôle de Château Gombert, zaabout.abdelghafour@yahoo.fr

†IUSTI Technopôle de Château Gombert

‡IUSTI Technopôle de Château Gombert

**Faculté des Sciences Tétouan : Mhannech II, B.

This paper is posted at ECI Digital Archives.

http://dc.engconfintl.org/fluidization_xiii/58

Characterization of turbulent regime behavior in the dilute zone of a circulating fluidized bed riser

Abdelghafour Zaabout^{a,b,*}, Hervé Bournot^a, René Occelli^a, Boussselham Kharbouch^b

^a IUSTI Technopôle de Château Gombert 5, rue Enrico FERMI 13453 Marseille cedex 13, France

^b Faculté des Sciences Tétouan : Mhannech II, B.P : 2121 Tétouan, Morocco

herve.bournot@univmed.fr, rene@polytech.univ-mrs.fr, kboussselham@yahoo.fr

* Corresponding Author. Mail: zaabout_abdelghafour@yahoo.fr. Tel : (+33)0611049166.

ABSTRACT

This study consists in characterizing the solid phase behavior in the dilute region of a circulating fluidized bed riser (CFB) for the turbulent regime (i.e. for superficial gas velocities $U_c < U_g < U_k$). Two sizes of particles (109 μm and 175 μm), and different static bed heights H_s (50 mm, 100 mm and 150 mm) for each distribution of particle, have been studied. Transition velocities U_c and U_k , which delimit the turbulent regime are determined from the standard deviation of the absolute pressure, and were found to increase with increasing H_s and not depend on axial positions. Radial profiles of the mean axial and transversal velocities have been determined with a PDA instrument. Two shapes of axial velocity profile (parabolic and concave) have been identified for the first distribution of particles (small particles). The shape is found to depend on the static bed height and the superficial gas velocity. Parabolic profiles were always found for the second distribution (large particles). The transversal velocities show that the particles move toward the riser center for small static bed heights H_s in the turbulent regime. This movement change toward the wall with increasing H_s , especially in the near wall region. More attention has been paid to the fluctuating character of the solid phase in analyzing the standard deviation of the mean axial and transversal particle velocities.

Keywords: Circulating fluidized bed; Turbulent regime; Transitions velocities; Phase Doppler Analyzer; Axial Particle velocity; transversal Particle velocity; fluctuating character.

INTRODUCTION

Recently and for several decades, characterization and determination of the different fluidization regimes existing in a CFB, is one of the most studied subject through the fluidization community (Bi and Grace (1); Monazam et al.(2)). The transition from the bubbling or (the slugging) regime to the transport regime is the most delicate point and has been discussed and studied by various authors (Rhodes (3); Bi et al. (4); Grace (5); Makkawi and Wright (6); Andreux et al. (7)). There is now a general consensus that the turbulent regime begins at U_c and ends at U_k . These two transition velocities U_c and U_k are introduced by Yerushalmi and Cankurt (8): U_c is the superficial gas velocity at which the standard deviation of the absolute pressure fluctuations reaches a maximum; and U_k is the superficial gas velocity corresponding to the leveling-off of the standard deviation of absolute pressure fluctuations as U_g increases. Note that some authors consider that U_k is equivalent to the transport velocity, U_{tr} , which demarcates the transition to fast fluidization regime (Chehbouni et al. (9), Rhodes (3)).

The bottom bed behavior (dense zone) in the turbulent regime has been widely studied. Lancia et al. (10), found that the void fraction remains constant for $U_c < U_g < U_k$. Chehbouni et al. (9), found that for $U_g > U_c$ the phenomenon of bubbles

exploding, dominates over the phenomenon of coalescence marking the bubbling regime, until the complete disappearance of these bubbles. Makkawi and Wright (6), found that the maximum bubble velocity is reached for $U_g = U_c$. Zhu and Zhu (12), found the core-annulus structure in the dense bottom bed. Zhu et al. (13) have found that the ascending particle velocity increases in the center and the descending particle velocity increases downward at the wall, with increasing U_g . Ellis et al. (14) showed that the movement of solid particles near the wall is associated with a lower void fraction than in the center riser.

Less attention has been paid to the upper zone of the fluidization riser during the turbulent regime comparing to the bottom zone. The core-annulus structure was identified by Makkawi and Wright (6), from the solid hold up measurement. Van den Moortel et al. (15), determined the radial profiles of mean axial particle velocities in the dilute zone of a circulating fluidized bed, for superficial gas velocities between U_c and U_k . Typical particle velocity profiles characterized by a displacement of the maximum velocity from the center of the flow to the core-annulus transition zone were observed, leading to a concave like profile. This study was conducted for a static bed height $H_s=100$ mm, and two particles distributions (diameter 60 μ m and 120 μ m). They found that with increasing U_g , the degree of concavity increases, reaches a maximum, decreases gradually, then disappears for $U_g = U_k$. A question arises from this latter study: is the structure found characterizes the overall behavior of the solid phase in the dilute zone of a CFB during the turbulent fluidization regime?

Our study presents further investigations of different operating conditions such as the static bed height and the particle size in order to propose answers to this question. The radial profiles of mean axial and transversal particle velocities have been measured using a particle dynamic analyzer (PDA), for two distributions of particles. For each particle distribution, the transition velocities U_c and U_k delimiting the turbulent regime has to be determined first. Three static bed heights H_s have been studied: 50, 100 and 150 mm. After, a detailed study of the turbulent regime has been conducted: four superficial gas velocities in this regime have been studied ($U_c \leq U_g \leq U_k$). Some higher gas velocities $U_g > U_k$ have also been studied for comparison. We used the expression of the dimensionless velocity introduced by Van den Moortel et al. (15), to determine the concavity degree of the radial profile of axial particle velocities. Moreover, a particular attention has been paid to the fluctuating nature of the particle movement. The axial and transversal particle velocities have been measured. For distribution 2, the results of $H_s=50$ mm are not presented as the solid mass flux is very low in the studied zone for all superficial gas velocities tested.

MATERIAL AND METHODS

The fluidization loop used for the present work is depicted in fig. 1. This experimental set up has been described in detail in previous papers (Van den Moortel et al. (16); Van den Moortel et al. (15)). The fluidization riser is H=2 m height, with a square cross section (D=0.2 m). Glass spheres ($\rho_p=2400$ kg/m³) were used with two distributions: 107 μ m mean diameter (called distribution 1) and 175 μ m (called distribution 2). A particle dynamic analyzer PDA, supplied by Dantec Electronics Ltd. of Denmark, is used to measure the particle velocity. The principle of this technique, based on the analysis of the light signal reflected by the particles

passing by interference fringes of a control volume created by two laser beam, was described in detail in previous paper (Van den Moortel et al. (16)).

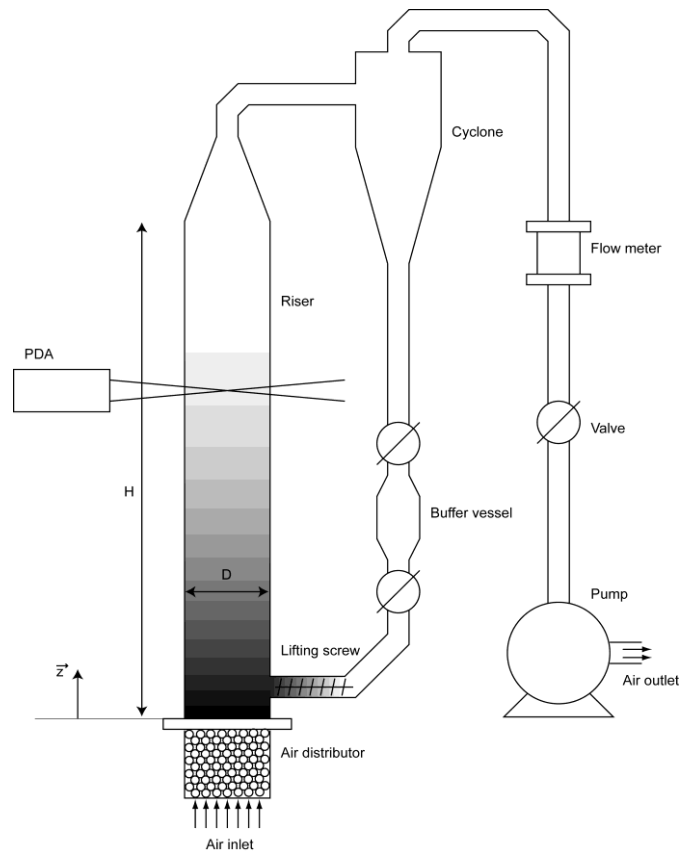


Fig.1. Schematic diagram of the circulating fluidized bed set up

RESULTS AND DISCUSSION

Identification of U_c and U_k

	H_s (mm)	U_c (m/s)	U_k (m/s)
$dp= 107 \mu\text{m}$	50	0.35	0.6
	100	0.56	0.78
	150	0.66	0.91
$dp= 175 \mu\text{m}$	100	0.66	0.92
	150	0.75	1.14

Tab.1. Transition velocities U_c and U_k for different static bed heights; distribution 1 and 2.

The absolute pressure fluctuations were measured at different axial locations above the bed surface, in order to determine the transition velocities U_c and U_k . The values of these transition velocities are reported in Tab. 1. For the two particle distributions, both U_c and U_k increase when increasing H_s , which is in agreement with previous results (Ellis et al., (14); Zhu et al. (13); Yang et Leu (11)). As expected, the two transition velocities U_c and U_k were found not depending on the axial position of the pressure probe.

Mean Particle Axial Velocity

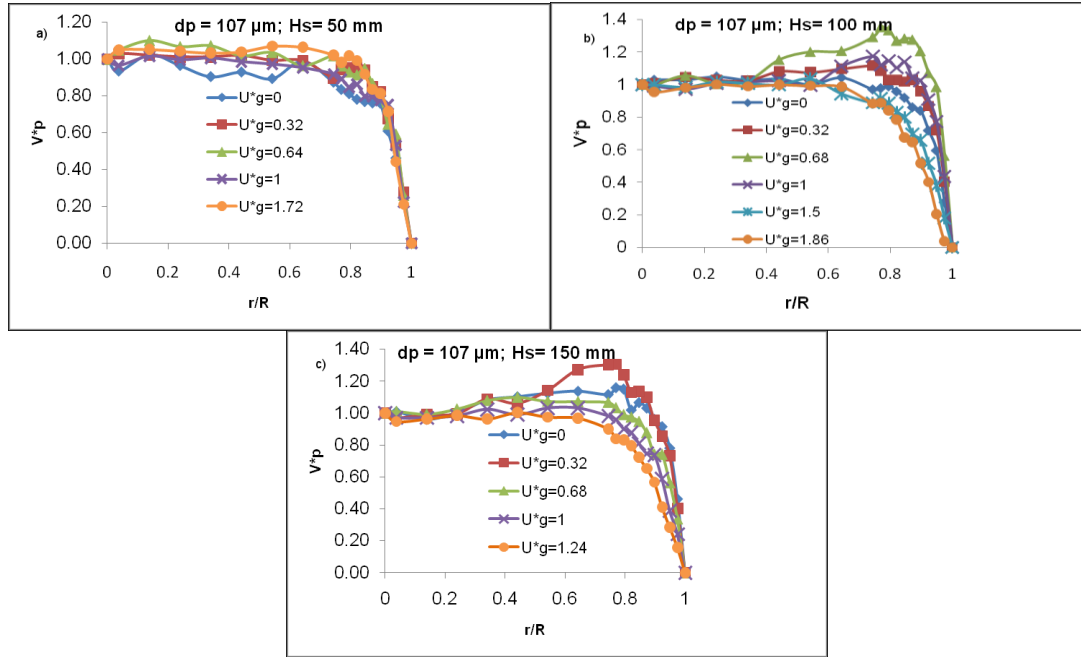


Fig.2. Evolution of the dimensionless axial particle velocity V_p^* as function of U_g^* . $d_p=107 \mu\text{m}$; $z/H=0.7$: a) $H_s=50 \text{ mm}$, b) $H_s=100 \text{ mm}$, c) $H_s=150 \text{ mm}$.

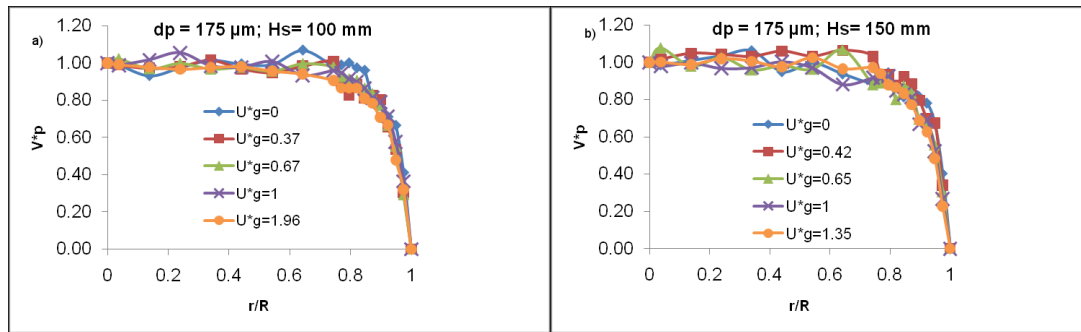


Fig.3. Evolution of the dimensionless axial particle velocity V_p^* as function of U_g^* . $d_p=175 \mu\text{m}$; $z/H=0.7$: a) $H_s=100 \text{ mm}$, b) $H_s=150 \text{ mm}$

For the sake of clarity, a dimensionless superficial gas velocity U_g^* is used (Eq. 1) so that the turbulent regime is defined by $0 \leq U_g^* \leq 1$ for each case of the previous tables. The fast fluidization regime starts when $U_g^* \geq 1$.

$$U_g^* = \frac{U_g - U_c}{U_k - U_c} \tag{1}$$

Only the half median plane of the riser is shown as the flow is symmetric. The radial coordinate is presented in dimensionless form r / R ($r / R = 0$ at the center of the riser and $r/R = 1$ at the wall). The measurement grid is refined at the wall in order to capture the velocity gradient which exists in this region.

The core-annulus structure is identified from the radial profiles of mean axial particle velocities (mean particle velocity negative near the wall and positive away from the

wall) for all operating conditions studied. Two types of profiles are brought out, which depend mainly on operating parameters: A concave shape appears on some profiles for high loaded conditions of distribution 1 ($H_s = 100$ mm, $H_s = 150$ mm) where the maximum of axial particle velocity is far from the center column (peak zone); A parabolic shape where the maximum of axial particle velocity is at the center of the column is found for the other operating conditions. There is a general trend for parabolic profiles: the mean axial particle velocity is increased upward in the center and downward in the wall with increasing U_g . For concave profiles, the same trend is found at the wall, but the increased mean axial particle velocity upward is observed at the core-annulus transition zone, not in the center riser.

In order to determine the conditions which lead the concave profile to appear and also to have a better overview of the “degree of concavity”, we choose to use a dimensionless expression introduced by Van den Moortel et al. (15). The axial velocity of particles at each position in the horizontal section is compared with its values at the center and at the wall as defined in Eq. (2).

$$V_p^*(r/R) = \frac{V_{pax}(r/R) - V_{pax}(r/R=1)}{V_{pax}(r/R=0) - V_{pax}(r/R=1)} \quad (2)$$

Thus if $V_p^*(r/R)$ stays lower than 1 the profile is called parabolic, and if $V_p^*(r/R)$ became greater than 1 we can say that a “concavity” exists.

The evolution of V_p^* as a function of the dimensionless superficial gas velocity U_g^* is shown in Fig. 2 and 3. Two completely different profiles can now be clearly identified. Concave profiles appear only for distribution 1 ($d_p = 107$ μ m) and for two static bed heights, $H_s = 100$ mm and $H_s = 150$ mm. They show a strong dependency on U_g^* . For $H_s=100$ mm of distribution 1, a very low concavity appears for $U_g^* = 0.32$, amplifies when increasing U_g^* , reaches a maximum ($V_p^*=1.4$ for $U_g^*=0.68$) and then decreases but still exists for $U_g^*=1$ ($U_g = U_k$). It disappears only when ending the turbulent regime for $U_g^* > 1$ and the profile becomes parabolic when increasing U_g^* furthermore. For $H_s=150$ mm, the same behavior is obtained but with a concavity which already appears for $U_g^*=0$, reaches a maximum for $U_g^* = 0.32$ and nearly disappears for $U_g^* = 1$.

Parabolic profiles are obtained for $H_s=50$ mm of distribution 1 and for both cases of distribution 2, and they are very U_g^* non-dependent when represented with the dimensionless expression of equation 2.

The vertical position has been suspected to play a role in the existence of this “concave” zone, but we verified that the concavity of the profile exists also on other relative heights of the riser.

The analysis of the mean dimensionless velocity profiles V_p^* versus U_g^* for different bed heights and two different distributions leads us to some questions. Within the well-defined (in terms of pressure fluctuations) turbulent regime of one particular distribution, one can obtain two different behaviors of the solid phase. It is, at this stage, difficult to interpret the causes of the velocity profiles “distortions” which lead to a concave shape, but the dense zone can reasonably be incriminated. Some authors suggest the influence of the drop bed vs. pressure drop distributor ratio on the quality of the fluidization in the dense zone and especially in the bubbling regime (Bonniol et al. (17)). Svensson et al. (18), showed a transition of the bottom bed

dynamics that goes from a “multiple bubble regime” for high pressure drop distributors to a “single bubble regime” otherwise. Therefore, the coupling between the dense zone in the bottom of the bed and the dilute zone above has to be intensely investigated to understand the origin of the development of the concave profile.

Mean Particle Transversal Velocity

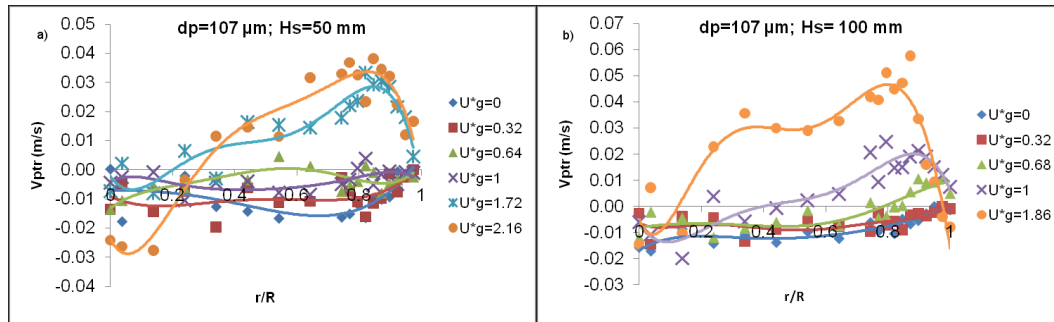


Fig.4. Evolution of mean transversal particle velocity as function of U_g . $d_p=107 \mu\text{m}$; $z/H=0.7$: a) $H_s=50 \text{ mm}$, b) $H_s=100 \text{ mm}$

The radial profiles of mean transversal particle velocities are shown on Fig.4, it brings information on the movement of the particles: negative sign of V_{ptr} means that the average movement of the particles is directed towards the center of the column, and positive sign toward the wall. Mean transversal particle velocities depend strongly on static bed height. For $H_s=50 \text{ mm}$, turbulent regime is characterized by a particle movement directed toward the center of the column. This movement, changes radically for $U_g^* > 1$ on almost the entire half-section of the column, except in the center where the movement of the particles has an opposite direction. For $H_s=100 \text{ mm}$ and 150 mm , the particle movement is also directed toward the center of the column for low superficial gas velocities; a small area appears near the wall where the particle movement is directed toward the wall when increasing U_g ; the thickness of this area increases with U_g and becomes major for $U_g^* > 1$.

Standard Deviation of Axial and Transversal Particle Velocity

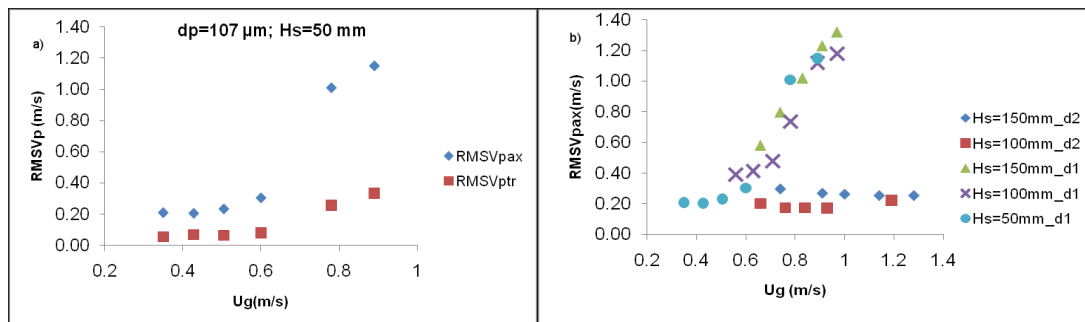


Fig.5. Standard deviation of mean particle velocity as a function of U_g at the center riser ($r/R=0$): a) Comparison of $RMSV_{pax}$ and $RMSV_{ptr}$; b) $RMSV_{pax}$ for both distribution 1 and 2.

Typical radial profiles are found for both $RMSV_{pax}$ and $RMSV_{ptr}$: constant value in the core, slight increase in the core-annulus transition zone, and decrease at the wall. Evolutions of $RMSV_{ptr}$ and $RMSV_{pax}$ values with U_g at the center riser have the

same shape for all static bed heights, but with higher values and magnitude for $RMSV_{pax}$ (Fig. 5a). On Fig. 5b), $RMSV_{pax}$ values at the center riser, are plotted as a function of the superficial gas velocity U_g ranging from turbulent to fast fluidization regime. A completely different evolution is observed between distribution 1 and 2. $RMSV_{pax}$ of distribution 2 is nearly constant. $RMSV_{pax}$ of distribution 1 shows clearly an S-like evolution for both $H_s=50$ mm and 100 mm; for $H_s=150$ mm, it seems quasi-linear with a slight decrease of the slope when attaining the fast fluidization regime.

CONCLUSION

PDA experiments has been conducted to characterize the solid phase behavior in the dilute region of a CFB riser for a superficial gas velocity in the range $U_c < U_g < U_k$ (turbulent regime). Some higher superficial gas velocities have also been investigated for comparison. Two sizes of particle (109 μm and 175 μm) and different static bed heights H_s (50 mm, 100 mm and 150 mm) have been studied.

The transition velocities U_c and U_k , which delimit the turbulent regime, were determined from the standard deviation of the absolute pressure and were found to increase when increasing H_s and independent on the axial position. Two shapes of axial particle velocity profile have been identified for the first distribution (small particles): a “parabolic” shape, and a “concave” shape. Parabolic profiles were found for the second distribution (large particles). In general, for parabolic profiles, increasing the superficial gas velocity increases the mean axial particle velocity upward in the center and downward at the wall. For concave profiles, increasing the superficial gas velocity increases the mean axial particle velocity upward in the peak zone and downward at the wall. The radial profile of mean particle transversal velocity has shown that particles move toward the riser center for the small static bed height H_s , in the turbulent regime. This movement change towards the wall with increasing H_s , especially near the wall.

The standard deviation of particle velocities presents different behaviors depending on the static bed height and the particle size. Axial and transversal standard deviations of particle velocities show a similar evolution with the superficial gas velocity.

NOTATION

D	diameter of the fluidization column, m
d_1	distribution 1
d_2	distribution 2
d_p	mean particle diameter, μm
H_s	static bed height, mm
PDA	Phase Doppler Analyzer
R_c	bed column radius, m
r	radial coordinate, m
$RMSV_{pax}$	standard deviation of mean particle axial velocity, m/s
$RMSV_{ptr}$	standard deviation of mean particle transversal velocity, m/s
U_g	superficial gas velocity, m/s
U_c	transition velocity from bubbling to turbulent regime, m/s
U_k	transition velocity from turbulent to fast fluidization regime, m/s
U_g^*	dimensionless velocity of U_g (Eq. 1)
V_{pax}	mean particle axial velocity, m/s
V_{ptr}	mean particle transversal velocity, m/s
V_p	dimensionless axial particle velocity (Eq. 2)

V_{pmax}^*	maximum of the dimensionless axial particle velocity
z/H	relative height of the fluidization column
ρ_p	particle density, kg/m ³

REFERENCES

- (1) Bi, H.T., Grace, J.R., 1995. Flow regime diagrams for gas-solid fluidization and upflow transport, *Int. J. Multiphase Flow* 21(6), 1229-1236.
- (2) Monazam, E. R., Shadle, L.J., Mei, J. S., Spenik, J., 2005. Identification and characteristics of different flow regimes in a circulating fluidized bed. *Powder Technology* 155, 17 – 25.
- (3) Rhodes, M., 1996. What is turbulent fluidization?. *Powder Technology*, 3-14.
- (4) Bi, H. T., Ellis, N., Abba, I. A., Grace, J. R., 2000. A state-of-the-art review of gas-solid turbulent fluidization, *Chemical Engineering Science* 55, 4789-4825.
- (5) Grace, J. R., 2000. Reflections on turbulent fluidization and dense suspension upflow. *Powder Technology* 113, 242–248.
- (6) Makkawi, Y. T., Wright, P. C., 2002. Fluidization regimes in a conventional fluidized bed characterized by means of electrical capacitance tomography, *Chemical Engineering Science* 57, 2411 – 2437.
- (7) Andreux, R., Gauthier, T., Chaouki, J., Simonin, O., 2005. New Description of Fluidization Regimes. *AIChE J* 51, 1125–1130.
- (8) Yerushalmi, J., Cankurt, N.T., 1979. Further Studies of the Regimes of Fluidization. *Powder Technology* 24, 187-205.
- (9) Chehbouni, A., Chaouki, J., Guy, C., Klvana, D., 1994. Characterization of the flow transition between bubbling and turbulent fluidization. *Industrial and Engineering Chemistry Research* 33, 1889-1898.
- (10) Lancia, A., Nigro, R., Volpicell, G., 1988. Transition from Slugging to Turbulent Flow Regimes in Fluidized Beds Detected by Means of Capacitance Probes. *Powder Technology* 56, 49 – 56.
- (11) Yang, T.-Y., Leu, L.-P., 2008. Study of transition velocities from bubbling to turbulent fluidization by statistic and wavelet multi-resolution analysis on absolute pressure fluctuations. *Chemical Engineering Science* 63, 1950 – 1970.
- (12) Zhu, H., Zhu, J., 2008. Characterization of fluidization behavior in the bottom region of CFB risers. *Chemical Engineering Journal* 141, 169–179.
- (13) Zhu, H., Zhu, J., Li, G., Li, F., 2008. Detailed measurements of flow structure inside a dense gas–solids fluidized bed. *Powder Technology* 180, 339–349.
- (14) Ellis, N., Bi, H.T., Lim, C.J., Grace, J.R., 2004. Hydrodynamics of turbulent fluidized beds of different diameters. *Powder Technology* 141, 124– 136.
- (15) Van den Moortel, T., Azario, E., Santini, R., Tadrst, L., 1998. Experimental analysis of the gas-particle flow in a circulating fluidized bed using a phase Doppler particle analyzer. *Chemical Engineering Science* 53, 1883-1899.
- (16) Van den Moortel, T., Seguin, P., Tadrst, L., 1999. Experimental analysis of the particle velocity profiles in the dilute zone of a fluidized bed. Transition from bubbling to turbulent regimes. In: Werther, J. (Ed), *Proceedings of the 6th International Conference on Circulating Fluidized Beds*. Dechema e.V., Würzburg, pp. 113-118.
- (17) Bonniol, F., Sierra, C., Occelli, R., Tadrst, L., 2000. Similarity in dense gas–solid fluidized bed, influence of the distributor and the air-plenum. *Powder Technology* 189, 14–24.
- (18) Svensson, A., Johnsson, F., Leckner, B., 1996. Fluidization regimes in non-slugging fluidized beds: the influence of pressure drop across the air distributor. *Powder Technology* 86, 299–312.